Available online at http://scik.org

J. Math. Comput. Sci. 11 (2021), No. 1, 543-562

https://doi.org/10.28919/jmcs/5101

ISSN: 1927-5307

THE FLOW BEHAVIOUR OF BLOOD IN TWO-PHASE TIME-DEPENDENT TAPERED STENOSED ARTERY IN THE PRESENCE OF TRANSVERSE MAGNETIC FIELD

B. S. VEENA*, ARUNDHATI WARKE

Symbiosis Institute of Technology (SIT), Symbiosis International (Deemed University),

Lavale, Pune - 412 115, Maharashtra State, India

Abstract: In this study, a tapered stenosed artery is considered to notice the effect of transverse magnetic field applied on blood flow to analyze the behavior of the flow with the help of significant flow attributes. The laminar, incompressible and fully developed flow of blood is studied taking into account the variable viscosity. To resemble the problem to real life situation, flow in core region is assumed to be non-Newtonian and flow in peripheral region is assumed to be Newtonian. The constitutive equation of blood is represented by Bingham plastic model in peripheral region and Herschel–Bulkley model in core region. The simulations are carried out for important flow characteristics such as wall shear stress, volumetric flow rate and axial velocity and the behavior is analyzed. We have reported numerical results for different values of physical parameters of interest. Biological implications of the present model are discussed. It has been observed that the important flow attributes are affected in tapered artery with stenosis and it is possible to stabilize the flow with the help of magnetic field applied externally. It is also noticed that the behaviour of flow attributes found by considering variable viscosity is in good agreement with the literature as compared to constant viscosity.

Keywords: two-fluid model; tapered artery; magnetic field; blood flow; stenosis.

2010 AMS Subject Classification: 35N05, 76W05.

*Corresponding author

E-mail address: veena@sitpune.edu.in

Received October 11, 2020

1. INTRODUCTION

The thickening of an artery is one of the initial stages of atherosclerosis which results in stenosed artery. As a result of stenosis developed in the artery, blood flow is disturbed. The serious consequences are the reduction of blood flow and increased resistance [5]. Blood is an electrically conducting fluid and strong magnetic field induces magnetization in blood. Magnetic field enhances unsteadiness in blood flow. Hence, there is influence of hematocrit, shape of artery and magnetic field on blood flow [16, 21]. The rheological behavior of blood is complex as compared to the behavior of simple fluids. Further, it is observed that the relation between shear rate and shear stress is important in understanding the nature of blood flow [7]. Hence, the modeling of non-Newtonian time dependent blood flow is feasible only with the aid of higher order differential equations [6, 20]. A model was developed by considering blood as laminar, incompressible and fully developed viscous fluid and observed that flow characteristics are noticeably influenced in the presence of uniform and spatially varying magnetic field, mostly by gradient and strength [17]. In highly stenosed arteries, flow rate decreases with increase in Hartmann number and stenosis height. It is also noticed that shear stress soars as stenosis height rises [9]. The axial velocity decreases towards the walls of artery. Studies on this topic revealed that flow is influenced strongly by ratio of radius of un-constricted part to maximum height of stenosis, yield stress and magnetic field. The flow is significantly influenced by increase in the level of hematocrit and magnetic field [8, 12]. All the flow attributes are influenced by magnetic field with different intensities in multi stenosed non-tapered artery and non-Newtonian rheology affects the attributes of the flow. It is also observed that, flow pattern changes as wall shear stress increases in non-Newtonian rheology, as compared to the results of Newtonian rheology [18]. Laplace and finite Hankel transforms are used to get the clear-cut information based on mathematical analysis to decide the level of shear stress that a patient can put up with if magneto therapy is used [15]. It is observed that, as gradient of magnetic field and percentage of hematocrit increases, effective viscosity increases. Further, as gradient of magnetic field and level of hematocrit increases, flow rate and axial velocity reduces gradually [2]. The stenosis height and yield stress have a strong influence on the characteristics of

blood flow both qualitatively and quantitatively. Due to multiple stenosis formation in arterial system, there is a barrier in fluid movement. The model thus developed may shed a light on clinical treatment of such hurdle and assists to lower at least few complications of ischemia and coronary thrombosis. The mathematical study of bell-shaped stenosis in a narrow artery using Casson fluid model shows that there is a rise in skin friction and flow resistance with maximum height of stenosis whereas increase in yield stress results in the decrease in these parameters [22]. The mathematical model implemented in coronary artery used experimental data and is able to apprehend the development of plaque qualitatively in the intima layer [3]. One-phase and two-phase models are used to study the effect of magnetization and found that shear stress in walls, longitudinal impedance and plug core radius are less in two-phase Herschel-Bulkley model as compared to the results of one-phase Herschel-Bulkley model [14]. An extensive quantitative study is carried out and found that as consistency of peripheral layer fluid decreases, mass-flux reduces and it is because of pseudo plastic nature of blood [13].

It is known that in large arteries, blood behaves like a non-Newtonian fluid in diseased conditions. It is reveled in many experimental studies that the shear rate is low in the territory of a stenosis and consequently the non-Newtonian behavior is quite prominent in stenosed area [10, 11]. Also, blood being non-Newtonian, its viscosity is not consistent. In this case, viscosity changes with shear rate, inversely or directly, depending upon whether fluid is shear thinning or shear thickening. As blood is shear thinning liquid, viscosity of blood is inversely proportional to shear rate, hence in core region, it is not a constant. Since blood behaves differently in peripheral and core regions, As H-B fluid model is preferable for low shear rate and characterizes reasonably what is occurring in blood, H-B model is used in core region. In addition to this, the constitutive equation of this model has an additional parameter as compared to any other non-Newtonian model which helps to obtain more detailed information. In addition to this, in peripheral region, Bingham plastic model is used.

The study of blood flow is important as it is more relevant in medical field and hence to understand the causes of circulatory disorders, it is essential to mathematically analyze fluid dynamical

properties of blood flow through the stenosed artery.

In this study, an unsteady two-dimensional analysis of blood flow through tapered stenosed vessel in the presence of magnetic field is investigated using a two-fluid model for constant and variable viscosity. To enhance the resemblance to the actual condition, the viscosity of blood depending on the percentage volume of erythrocytes is considered while analyzing the flow.

The main focus of this study is to find the outcome of transverse magnetic field applied externally on blood flow in tapered stenosed artery. Many parameters affect blood flow. In the present study, the expressions for axial velocity, volumetric flow rate, and wall shear stress are the key features in analyzing blood flow. The effect of yield stress, height of stenosis and magnetic field have been studied exclusively, through which the relationship between arterial wall biology, biomechanics and geometric complexities can be apprehended. Thus, this study plays a major role in interpreting the links between arterial disease and biomechanics.

2. PROBLEM FORMULATION

The schematic representation of a tapered two-fluid model with mild stenosis is shown in Fig. 1. For non-tapered artery $\varphi = 0$ and for tapered artery $\varphi \neq 0$, in particular for converging artery $\varphi < 0$ and for diverging artery $\varphi > 0$ where φ is tapering angle.

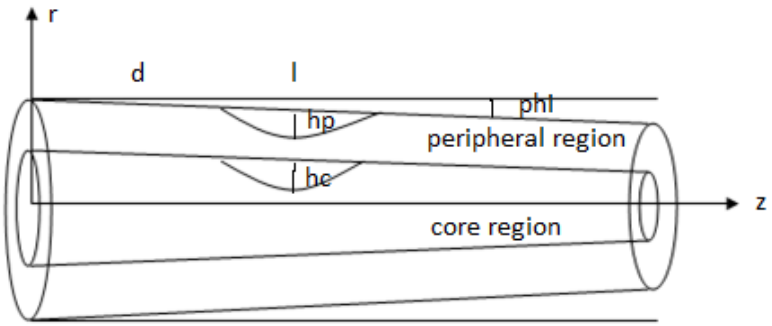

Fig. 1. Schematic representation of tapered two-fluid model

The problem is formulated mathematically based on the assumptions that blood is incompressible, viscous and non-homogeneous; flow is unsteady, fully developed and two-dimensional; negligible electric field. There is no external electric field and no induced magnetic field but a transverse magnetic field is applied externally.

Using the dimensionless scheme, the system of equations is converted to a non-dimensional form. The mathematical equations of two-fluid model in peripheral and core region respectively are given by

$$R_p(z,t) = \left\{(R_0 + md) + \left[m - \left(\frac{hp}{l}\right)\right](z-d) + \left(\frac{hp}{l^2}\right)\ (z-d)^2\right\} a(t) \quad (1)$$

where $d \ \leq z \leq \ d + l$

$R_p(z,t) = (mz + R_0)a(t)$ otherwise

$$R_c(z,t) = \left\{(R_c + md) + \left[m - \left(\frac{hc}{l}\right)\right](z-d) + \left(\frac{hc}{l^2}\right)\ (z-d)^2\right\} a(t) \quad (2)$$

where $d \ \leq z \leq \ d + l$

$R_c(z,t) = (mz + R_c)a(t)$ otherwise [19]

$$\text{where} \quad a(t) = 1 - b(\cos\ wt - 1)\, e^{-bt} \quad (3)$$

$\omega \ = 2\pi f_p$, f_p is pulse frequency, $b = 0.1$ for blood, a constant, $f_p \ = \ 1.2\, Hz$, $t \ =$ 0.1, 0.3, etc., and since 0.85 sec. is the time for one cardiac cycle, the maximum time for t is chosen to be 0.85 sec. Here $Rp \ \ (z \ \ ,t \ \ )$ and $Rc \ \ (z \ \ ,t \ \ )$ are radii of stenosed part of peripheral and core region respectively, R_0 and R_c are radii of un-constricted part of peripheral and core region respectively. hc is the height of stenosis in core region where as hp is the height of stenosis in peripheral region. Here $h_p \ = 4\, \tau_m\, sec\, \varphi = 4pR_p\ \sec\varphi$ and $h_c \ = 4\, \tau_m\, sec\, \varphi = 4pR_c\ \sec\varphi$ where p is a real number between 0 and 1. Stenosis is mild if $p <\ 0.4$, medium if $0.4 < p <\ 0.6$ and severe if $p >\ 0.6$ The angle of tapering φ is same in both the regions. However, the percentage of stenosis can be different in different regions. Also, $\gamma R_0 \ = R_c$, $R_p \ = R_0 \ - R_c$ and $R_p \ < R_c$ where γ = 0.95 to 0.98. i.e., peripheral region is a thin layer surrounding core region.

The governing equation satisfying all the conditions mentioned above is given by

$$-\frac{\partial P}{\partial z}+\frac{1}{r}\frac{\partial(r\tau)}{\partial r}+F\frac{dH}{dz}=0 \text{ where } F=\frac{kMH_0}{\rho u_0^2} \text{ , } F \text{ is called magnetic number. [1\}} \quad (4)$$

Here k is magnetic permeability, M is magnetization, H is magnetic field intensity, P is pressure and τ is shear stress.

The constitutive equation in core region is given by Herschel-Bulkley model [11]

$$\tau=\tau_c+\left[A\left(-\frac{\partial u}{\partial r}\right)\right]^{\frac{1}{n}} \text{ if } \tau\geq\tau_c$$

$$\frac{\partial u}{\partial r}=0 \text{ if } \tau<\tau_c \text{ where } n>1 \text{ or } n<1 \quad (5)$$

$$\text{where} \quad A=\frac{\mu}{\rho^{n-1}u_0^{2n-2}}=B\left[1+\beta.He\left\{1-\left(\frac{r}{R_c}\right)^q\right\}\right] \text{ and } B=\frac{\mu_0}{\rho^{n-1}u_0^{2n-2}} \quad (6)$$

In this model, viscosity may vary.

The constitutive equation in peripheral region is given by Bingham plastic model [4]

$$\tau=\tau_c+\left[C\left(-\frac{\partial u}{\partial r}\right)\right] \quad \text{if } \tau\geq\tau_c \text{ where} C=\mu, \text{a constant}$$

$$\frac{\partial u}{\partial r}=0 \text{ if } \tau<\tau_c \quad (7)$$

In this model viscosity is constant.

At the center of artery, the maximum hematocrit, $He = 20\%$ to 50%, μ_0 = viscosity of plasma = 1.3 to 1.8 cp, β = 2.5 for blood, τ_0 is yield stress which is essential to begin the flow.

Here the value of constant A depends on r and He (hematocrit) and other parameters are constants. He is different for different patients. However, He remains the same in a particular situation.

If the flow behavior index n is unity then the flow becomes Newtonian. Here $q \geq 2$ is the parameter to determine the exact shape of viscosity profile for blood. The shape of viscosity profile given in (6) is applicable only for dilute suspension of spherical shape erythrocytes.

Boundary conditions are given by

$$u=0 \text{ at } r=R_c(z,t) \text{ and } r=R_p(z,t); \quad \frac{\partial u}{\partial r}=0 \text{ and } \tau \text{ is finite at } r=0 \quad (8)$$

3. RESULTS AND DISCUSSION – CONSTANT VISCOSITY

3.1 Axial velocity

Consider μ = viscosity of blood = a constant

Using binomial expansion of (5) by neglecting higher terms and (4), we get,

$$\text{i.e.,} u = -\frac{1}{A}\left[\begin{array}{r}\left\{\frac{1}{2}\left(\frac{\partial P}{\partial z} - F\frac{dH}{dz}\right)\right\}^{n}\frac{R^{n+1}(z,t)-r^{n+1}}{n+1} - \tau_c\left\{\frac{1}{2}\left(\frac{\partial P}{\partial z} - F\frac{dH}{dz}\right)\right\}^{n-1}\left[R^{n}(z,t) - r^{n}\right] \\ +\frac{n}{2}\tau_c^2\left\{\frac{1}{2}\left(\frac{\partial P}{\partial z} - F\frac{dH}{dz}\right)\right\}^{n-2}\left[R^{n-1}(z,t) - r^{n-1}\right]\end{array}\right] \quad (9)$$

a) Core region $n \neq 1$

$$u_c = -\frac{1}{A}\left[\begin{array}{r}\left\{\frac{1}{2}\left(\frac{\partial P}{\partial z} - F\frac{dH}{dz}\right)\right\}^{n}\frac{R_c^{n+1}(z,t)-r^{n+1}}{n+1} - \tau_c\left\{\frac{1}{2}\left(\frac{\partial P}{\partial z} - F\frac{dH}{dz}\right)\right\}^{n-1}\left[R_c^{n}(z,t) - r^{n}\right] + \\ \frac{n}{2}\tau_c^2\left\{\frac{1}{2}\left(\frac{\partial P}{\partial z} - F\frac{dH}{dz}\right)\right\}^{n-2}\left[R_c^{n-1}(z,t) - r^{n-1}\right]\end{array}\right] \quad (10)$$

where r ranges from 0 to R_c

b) Peripheral region $n = 1$

$$u_p = -\frac{1}{A}\left[\left\{\frac{1}{4}\left(\frac{\partial P}{\partial z} - F\frac{dH}{dz}\right)\right\}\left[R_p^2(z,t) - r^2\right] - (R_p(z,t) - r)\tau_c + \tau_c^2\left(\frac{\partial P}{\partial z} - F\frac{dH}{dz}\right)^{-1}\right] \quad (11)$$

where r ranges from R_c to R_p.

The trend of axial velocity in different situations is presented below.

The variation in axial velocity in the core region in the diverging and converging artery for different magnetic field gradients is shown in Fig.2. It is observed that axial velocity decreases as r increases for a smaller value of magnetic field gradient. It is zero irrespective of the magnetic field gradient at $r = 0.12$ in converging and at $r = 0.2$ in the diverging artery. At high magnetic field gradient ($H = 40000$), axial velocity is almost stable in both cases. At $r = 0$, more variation in axial velocity can be observed in the diverging artery.

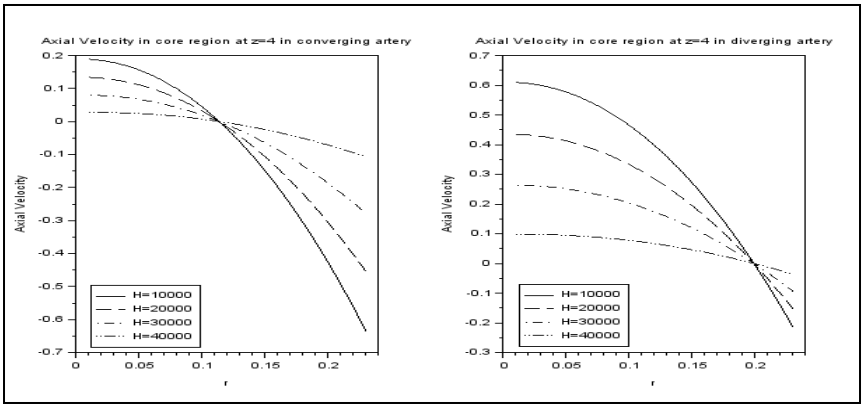

Fig. 2. Axial velocity in core region for different values of magnetic field gradient when $n = 1.05$

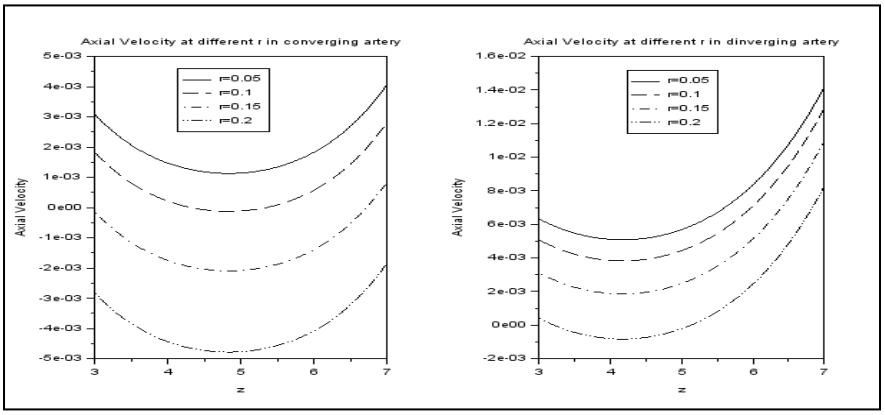

Fig. 3. Axial velocity in core region at different r when $n = 1.05$

Fig.3 depicts the profile of axial velocity in the core region at different r (radial coordinate). In the converging artery, as z increases from 3 to 5, axial velocity decreases uniformly and then increases uniformly. In case of the diverging artery, initially, there is a slight decrease in axial velocity up to $z = 4$ and then it increases drastically. Axial velocity is high near the center line of the artery.

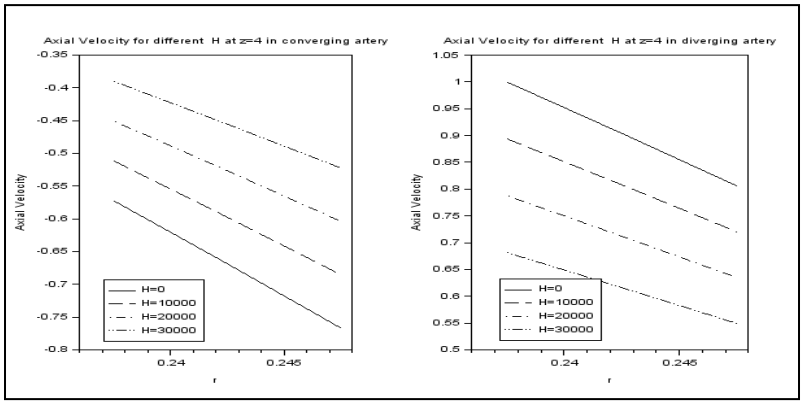

Fig. 4. Axial velocity in peripheral region for different magnetic field gradients when $n = 1.05$

Fig. 4 establishes the effect of a magnetic field gradient on axial velocity in the peripheral region for a fixed value of other parameters. Axial velocity decreases linearly as r increases. Higher values of axial velocity profile with increasing magnetic field gradient are observed in the converging artery and exactly opposite trend is observed in the diverging artery.

3.2 Volumetric flow rate

$$Q = 2\pi \int_0^{Rc(z,t)} r u_c dr + 2\pi \int_{Rc}^{Rp(z,t)} r u_p dr = Q_1 + Q_2 \quad (12)$$

where $Q_1 = \frac{-2\pi}{A}\left[\left\{\frac{1}{2}\left(\frac{\partial P}{\partial z} - F\frac{dH}{dz}\right)\right\}^n \left(\frac{R_c^{n+3}(z,t)}{2(n+1)} - \frac{R_c^{n+3}(z,t)}{(n+3)(n+1)}\right) - \tau_c \left\{\frac{1}{2}\left(\frac{\partial P}{\partial z} - F\frac{dH}{dz}\right)\right\}^{n-1} \left(\frac{R_c^{n+2}(z,t)}{2} - \frac{R_c^{n+2}(z,t)}{n+2}\right) + \frac{n}{2}\tau_c^2 \left\{\frac{1}{2}\left(\frac{\partial P}{\partial z} - F\frac{dH}{dz}\right)\right\}^{n-2} \left(\frac{R_c^{n+1}(z,t)}{2} - \frac{R_c^{n+1}(z,t)}{n+1}\right)\right]$ (13)

$$Q_2 = \frac{-2\pi}{A}\left[\left\{\frac{1}{4}\left(\frac{\partial P}{\partial z} - F\frac{dH}{dz}\right)\right\}\left(\frac{R_p^4(z,t)}{2} - \frac{R_p^2(z,t)R_c^2}{2} - \frac{R_p^4(z,t)}{4} + \frac{R_c^4}{4}\right) - \tau_c\left(\frac{R_p^3(z,t)}{2} - \frac{R_p(z,t)R_c^2}{2}\right) + \tau_c^2\left(\frac{\partial P}{\partial z} - F\frac{dH}{dz}\right)^{-1}\left(\frac{R_p^2(z,t)}{2} - \frac{R_c^2}{2}\right)\right] \quad (14)$$

The following figures depict the behavior of volumetric flow rate in different situations.

The variation in flow rate versus axial coordinate for a range of magnetic field gradients is shown in Fig.5. At the beginning of the converging artery, the flow rate is more as compared to the results.

This trend is reversed in the diverging artery. Flow rate attains its minimum at $z = 4.5$ in the converging artery and it attains its minimum at $z = 4$ in the diverging artery. The volumetric flow rate is the same at $z = 2.8$ and 6.8 irrespective of the magnetic field in the converging artery, this trend has not been observed in the diverging artery.

Fig. 6 explains the variations in flow rate for the set tapering angles in diverging and converging arteries. In the beginning, the fast decrease in flow rate in the converging artery as compared to the diverging artery has been observed. Later, the volumetric flow rate increases slowly in converging and faster in a diverging artery. The trend in the volumetric flow rate profile is reversed concerning the tapering angle.

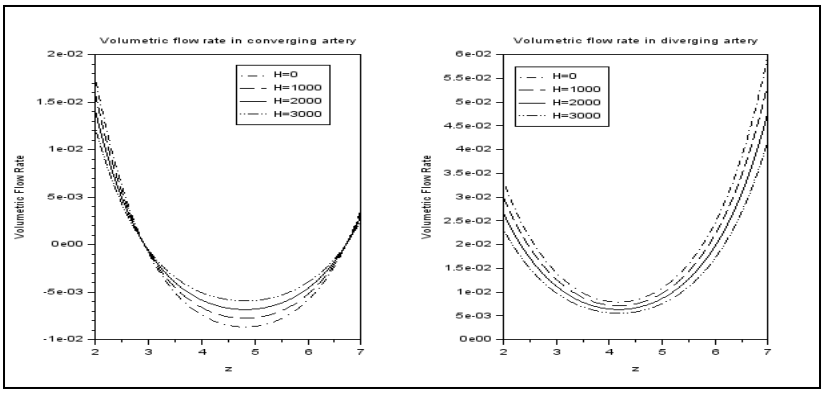

Fig. 5. Flow rate for different magnetic field gradients when $n = 0.95$

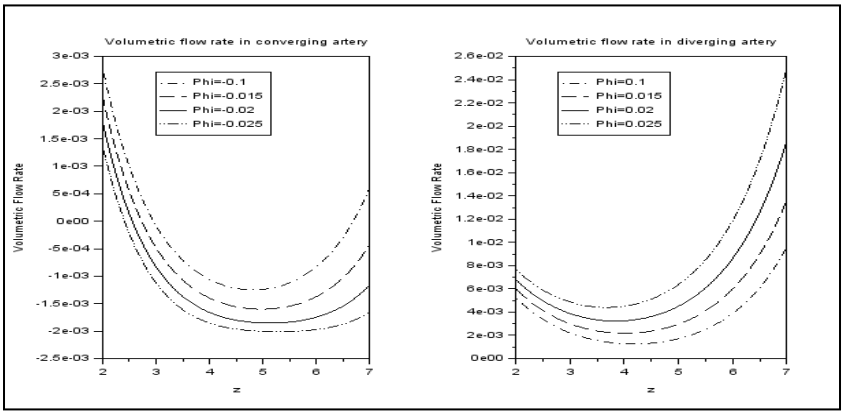

Fig. 6. Flow rate for different tapering angles when $n = 0.95$

Fig. 7 depicts the trend of volumetric flow rate with respect to magnetic number. As z increases, opposite trend in the profiles of flow rate can be observed in diverging and converging arteries. In case of converging artery, the flow rate is same at $z = 3$ and $z = 6$ irrespective of magnetic number which is not being seen in diverging artery. For higher magnetic number, stability in volumetric flow rate can be achieved.

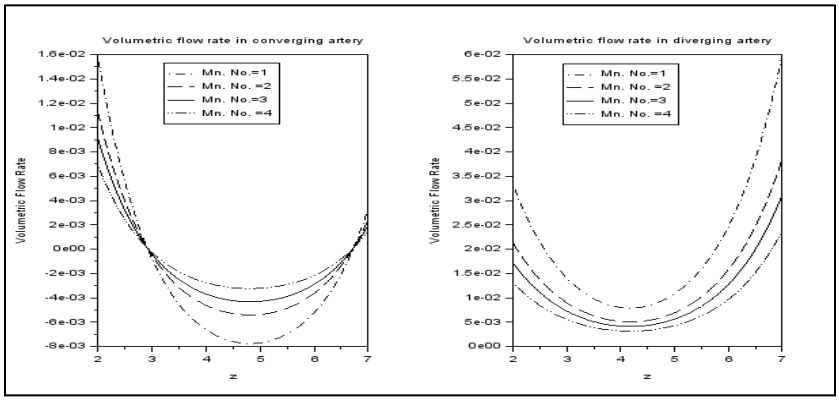

Fig. 7. Flow rate for different magnetic numbers when $n = 0.95$

Fig. 8 represents the profiles of wall shear stress against the axial coordinate. Initially, wall shear stress increases as z increases and then decreases along with the increase in z with different rates in diverging and converging arteries. From the figure, it is clear that as the gradient of magnetic field increases, wall shear stress increases.

3.3 Wall shear stress

The expression of wall shear stress is obtained as

$$\tau_w = 2\tau_c - \frac{1}{2}\left(\frac{\partial P}{\partial z} - F\frac{dH}{dz}\right)R_p(z,t) \tag{15}$$

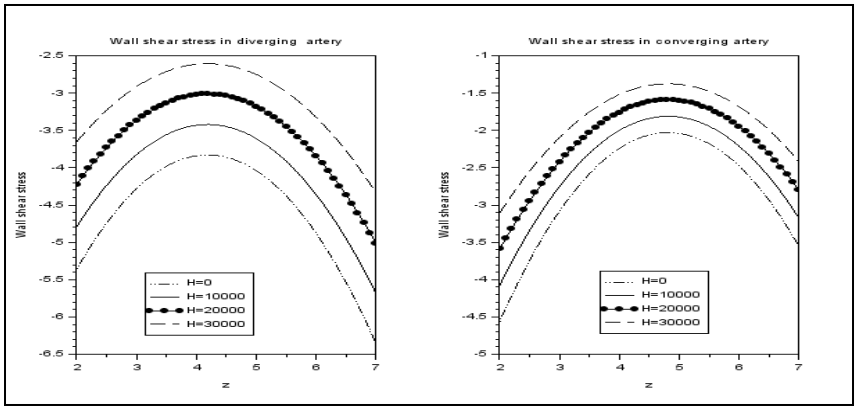

Fig. 8. Wall shear stress for different magnetic field gradients in diverging and converging artery when $n = 0.95$

4. RESULTS AND DISCUSSION - VISCOSITY IS VARIABLE

4.1 Axial velocity

Let viscosity be variable in core region and constant in peripheral region.

Using (4), (5) and (6), we get,

$$u_c = -\frac{1}{A}\left[\left\{\frac{1}{2}\left(\frac{\partial p}{\partial z} - F\frac{dH}{dz}\right)\right\}^n \frac{R_c^{n+1}(z,t) - r^{n+1}}{n+1} - \tau_c\left\{\frac{1}{2}\left(\frac{\partial p}{\partial z} - F\frac{dH}{dz}\right)\right\}^{n-1}\left[R_c^n(z,t) - r^n\right] + \frac{n}{2}\tau_c^2\left\{\frac{1}{2}\left(\frac{\partial p}{\partial z} - F\frac{dH}{dz}\right)\right\}^{n-2}\left[R_c^{n-1}(z,t) - r^{n-1}\right]\right] \quad (16)$$

where r ranges from 0 to Rc.

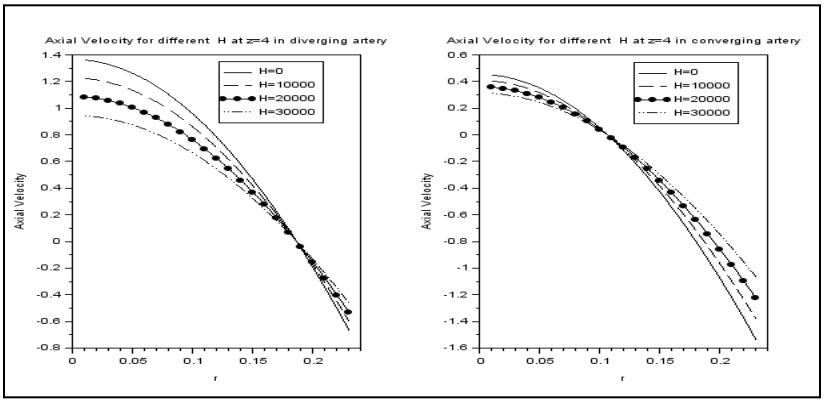

Fig. 9. Axial velocity in core region for different magnetic field gradients with variable viscosity

Since viscosity in the peripheral region is a constant, the variations in axial velocity in the peripheral region are same as discussed in the previous section. As viscosity varies with the position and percentage of hematocrit, more attention is given for the discussion of axial velocity in the core region. The following graphs depict the variations in axial velocity in different cases.

A comparison of velocity profiles in the diverging and converging artery is shown in Fig. 9. Here, viscosity changes with r, and hematocrit is constant. It can be noticed from the figure that axial velocity decreases as r increases. There is a significant change in axial velocity for the magnetic field in the diverging artery. Axial velocity, as well as the rate of fall in velocity profile, is more near the central line as compared to profiles of axial velocity with constant viscosity (Fig.3).

Fig. 10 exhibits the results for axial velocity in the core region with variable viscosity for different magnetic field gradients. In this case, viscosity varies with the position and not with hematocrit. As viscosity increases, axial velocity decreases. The rate at which the axial velocity decreases is more when blood is shear thickening than in case of shear thinning of blood. The increase in the magnetic field gradient is helping in decreasing the rate of change.

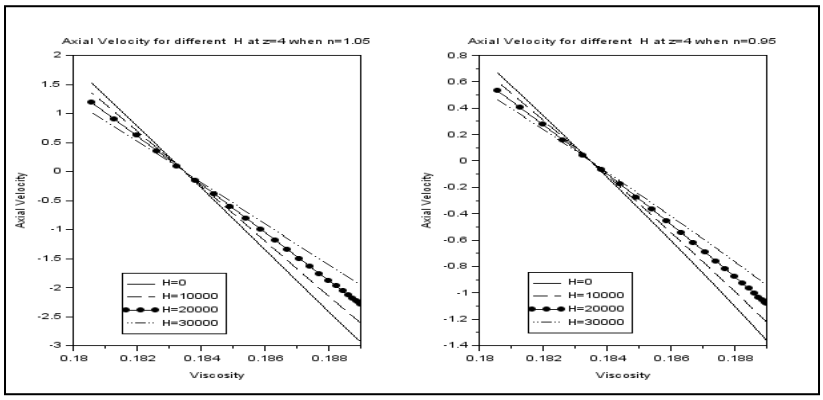

Fig. 10. Axial velocity in core region versus viscosity for different magnetic field gradients

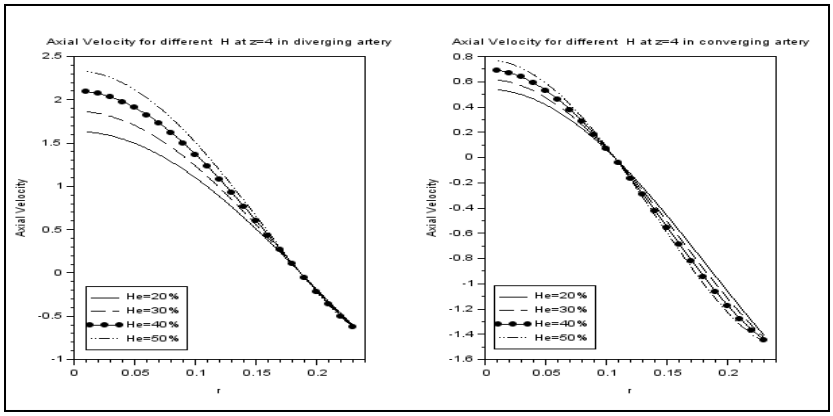

Fig. 11. Axial velocity in core region with r for different hematocrit at $z = 4$

Fig. 11 shows the trend of axial velocity for different percentage of hematocrit. Axial velocity decreases as r increases. A significant variation can be observed in the diverging artery for different values of hematocrit. However, in the converging artery, a slight change can be observed. The increase in hematocrit level helps in increasing axial velocity near the center line of the artery and as we move towards the peak of stenosis, axial velocity drops down to zero irrespective of the percentage of stenosis.

Fig. 12 illustrates the results for axial velocity in the core region with viscosity for different magnetic field gradients. Here viscosity depends on both position and hematocrit. Hematocrit is considered as $20\ \%, 30\ \%, 40\ \%$ and $50\ \%$ for $\frac{dH}{dz} (\approx \boldsymbol{H})$=0, 3000, 6000 and 9000 respectively. In both cases, a linear relationship between viscosity and velocity can be observed, and as viscosity increases, velocity decreases. It can be concluded that in the core region, proper application of magnetic field depending upon hematocrit and position of stenosis in patients, axial velocity can be stabilized.

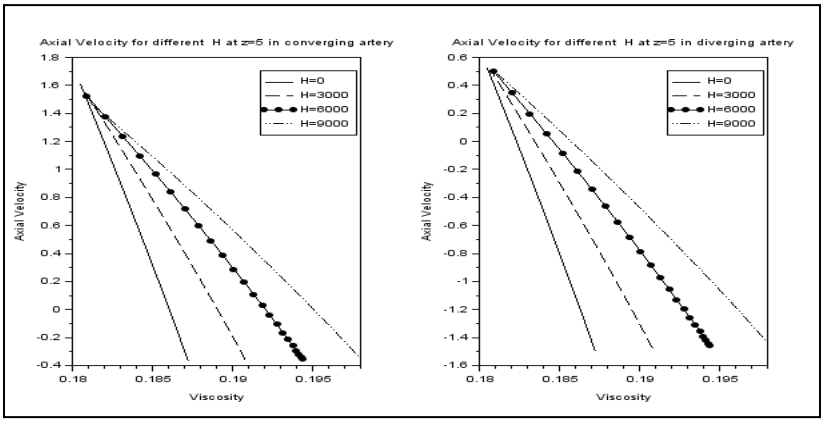

Fig. 12. Axial velocity in core region with viscosity for different magnetic field gradients at $z = 5$ in converging and diverging artery

3.4 Volumetric flow rate

Using expressions of axial velocity in core and peripheral region, expression for volumetric flow rate is derived as

$$Q \quad = 2\pi \int_0^{Rc(z,t)} r u_c dr + 2\pi \int_{Rc}^{Rp(z,t)} r u_p dr \quad = \quad Q_1 + Q_2 \tag{17}$$

$$Q_1 = -2\pi \int_0^{R_c(z,t)} r \left(-\frac{1}{A} \left[\left\{ \frac{1}{2} \left(\frac{\partial P}{\partial z} - F \frac{dH}{dz} \right) \right\}^n \frac{R_c^{n+1}(z,t) - r^{n+1}}{n+1} - \tau_c \left\{ \frac{1}{2} \left(\frac{\partial P}{\partial z} - F \frac{dH}{dz} \right) \right\}^{n-1} [R_c^n(z,t) - r^n] + \frac{n}{2} \tau_c^2 \left\{ \frac{1}{2} \left(\frac{\partial P}{\partial z} - F \frac{dH}{dz} \right) \right\}^{n-2} [R_c^{n-1}(z,t) - r^{n-1}] \right] \right) dr \tag{18}$$

This is an improper integral. Hence, the integral is evaluated using Simpson's 3/8th rule by dividing the interval $[0, R_c(z,t)]$ into large number of subintervals to make sure that the value of the integral is error free.

$$Q_2 = \frac{-2\pi}{\mu} \left[\left\{ \frac{1}{4} \left(\frac{\partial P}{\partial z} - F \frac{dH}{dz} \right) \right\} \left(\frac{R_p^4(z,t)}{2} - \frac{R_p^2(z,t) R_c^2}{2} - \frac{R_p^4(z,t)}{4} + \frac{R_c^4}{4} \right) - \tau_c \left(\frac{R_p^3(z,t)}{2} - \frac{R_p\,(z,t) R_c^2}{2} \right) + \tau_c^2 \left(\frac{\partial P}{\partial z} - F \frac{dH}{dz} \right)^{-1} \left(\frac{R_p^2(z,t)}{2} - \frac{R_c^2}{2} \right) \right] \tag{19}$$

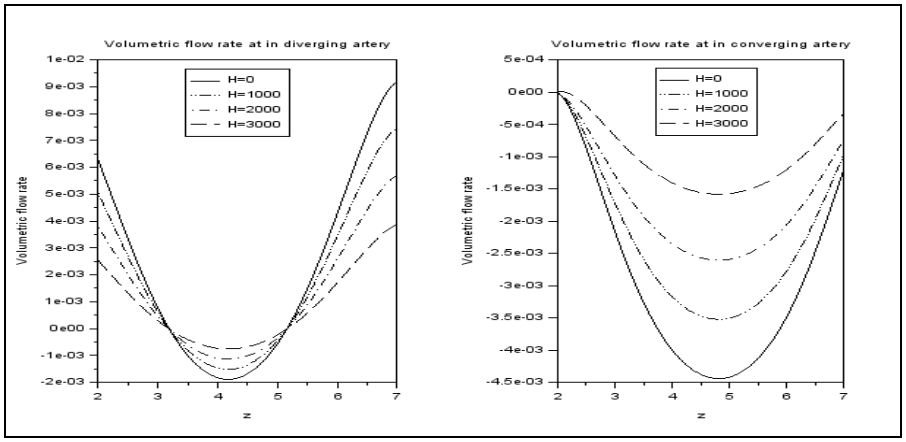

Fig. 13. Profile of flow rate for different magnetic field gradients when $n = 0.95$

Fig. 13 illustrates the behaviour of flow rate with variable viscosity for different magnetic field gradients in both diverging and converging artery when $n = 0.95$. Here, we have assumed that viscosity varies with the position (r). Flow rate drops in the first half of stenosis and it increases in the next half. In the diverging artery, the flow rate is less in the beginning as compared to the later part which is not being seen in the converging artery. A twist in the profile has been observed between $z = 3$ and 5.2 in the diverging artery. Proper application of the magnetic field can stabilize the flow rate. However, there is no notable change in the behaviour of flow rate when viscosity varies with hematocrit along with r which is not shown in the figure here.

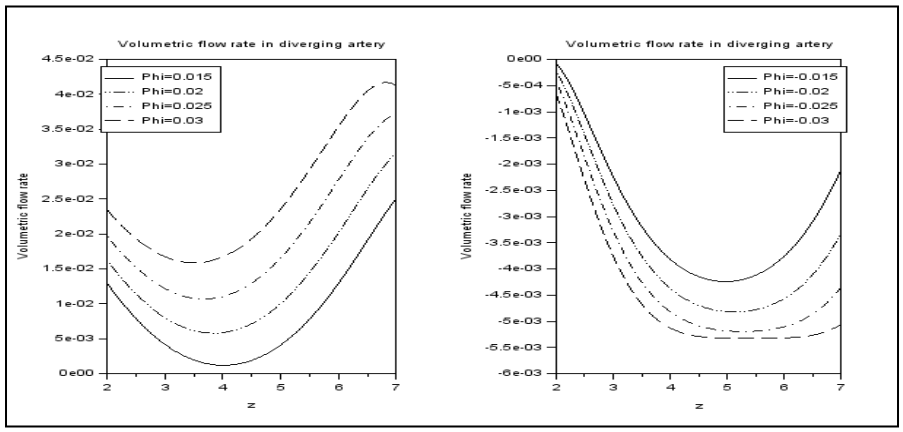

Fig. 14. Volumetric flow rate for different tapering angles when $n = 1.05$

Again, viscosity is allowed to vary with the position and hematocrit while calculating the volumetric flow rate for different tapering angles, and the profile is shown in Fig. 14. As z increases, the flow rate decreases initially and then increases. However, the rate is different as well as the point at which it is minimum in both diverging and converging artery. But in the converging artery, the difference in flow rates at the ends is more as compared to the diverging artery.

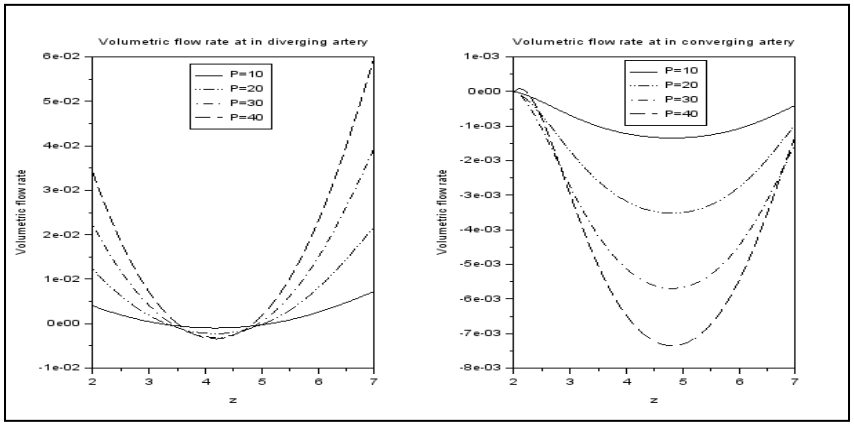

Fig. 15. Volumetric flow rate for different pressure gradients when $n = 1.05$

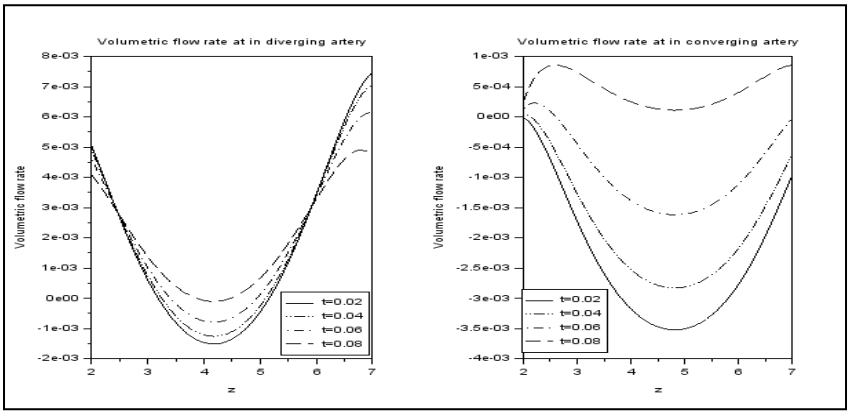

Fig. 16. Volumetric flow rate for different yield stress when $n = 0.95$

Fig. 15 illustrates the profile of the volumetric flow rate for different pressure gradients with variable viscosity, hematocrit and position of stenosis by keeping other parameters constant. It is observed that in the diverging artery, as pressure gradient increases, variation in flow rate increases and flow rate decreases in the converging artery. The flow rate in the diverging artery is the same in the middle of stenosis irrespective of the pressure gradient. The flow rate attains stability with a higher-pressure gradient.

It is observed from Fig.16 that yield stress is also an important factor in regulating the volumetric flow rate when viscosity is variable. When yield stress is less, the variation in the volumetric flow rate is more. As we increase yield stress, variation in flow rate decreases. A twist in the profile of the flow rate is observed in the diverging artery. Also, it can be observed that when yield stress is more, volumetric flow rate does not follow any specific pattern.

5. CONCLUSION

A two-dimensional analysis of the unsteady flow of blood through a stenosed tapered artery with constant/variable viscosity in the presence of a magnetic field has been carried out. A two-layered model, the inner (core) region consisting of erythrocytes is assumed to follow the Herschel-Bulkley fluid model (blood is non–Newtonian) and the outer (peripheral) region near the wall of the artery, as Bingham plastic fluid model (similar to Newtonian but with yield stress). To resemble a real-life situation, the viscosity of blood is assumed as (i) constant (ii) variable whereas in the second case, viscosity is allowed to vary with shear rate. Expressions for wall shear stress, volumetric flow rate, and axial velocity have been derived using a combination of numerical and analytical methods. Variations in pressure gradient, magnetic field, tapering angle, etc., are taken into account to analyze the results with the help of graphs drawn using Scilab.

It is found that the shape of the artery, tapering angle, magnetic field gradient, pressure gradient, viscosity, yield stress, the intensity of the magnetic field, type of stenosis – height, place, and percentage of stenosis are the key factors which prompts the flow. These parameters help to

stabilize the flow and is visualized in the graphs. It is further noticed that the proper application of magnetic field with appropriate pressure can regulate the flow significantly.

CONFLICT OF INTERESTS

The authors declare that there is no conflict of interests.

REFERENCES

[1] R. Bali, U. Awasthi, A Casson fluid model for multiple stenosed artery in the presence of magnetic field, Appl. Math. 3(5) (2012), 436-441.

[2] R. Bali, U. Awasthi, Mathematical model of blood flow in small blood vessel in the presence of magnetic field, Appl. Math. 2(2) (2011), 264-269.

[3] M. Cilla, E. Peria, M. A. Martinez, Mathematical modeling of atheroma plaque formation and development in coronary arteries, J. R. Soc. Interface. 11(90) (2014), 20130866.

[4] R. P. Chhabra, J. Richardson, Non-Newtonian flow and applied rheology: Engineering applications, Elsevier, (2008).

[5] S. Chakravarty, Effects of stenosis on the flow-behavior of blood in an artery, Int. J. Eng. Sci. 25(8) (1987), 1003-1016.

[6] J. Enderle, B. Susan, B. Bronzino, Introduction to biomedical engineering, Academic Press, London, (2000).

[7] R. L. Fournier, Basic transport phenomena in biomedical engineering, Taylor and Francis, (1998).

[8] M. Jain, G. C. Sharma, R. Singh, Mathematical modelling of blood flow in a stenosed artery under MHD effect through porous medium, Int. J. Eng. Trans. B, Appl. 23(3-4) (2010), 243-251.

[9] S. Kumar, S. Kumar, D. Kumar, Oscillatory MHD flow of blood through an artery with mild stenosis. IJE Transactions A: Basics 22(2) (2009), 125-130.

[10] P. K. Mandal, An unsteady analysis of non-Newtonian blood flow through tapered arteries with a stenosis, Int. J. Non-Linear Mech. 40(1) (2005), 151-164.

[11] J. C. Misra, G. C. Shit, Role of slip velocity in blood flow through stenosed arteries: a non-Newtonian model, J. Mech. Med. Biol. 7(3) (2006), 337-353.

[12] J. C. Misra, A. Sinha, G. C. Shit, Mathematical modeling of blood flow in a porous vessel having double stenosis in the presence of an external magnetic field, Int. J. Biomath. 4(2) (2011), 207-225.

[13] G. Neeraja, P. A. Dinesh, K. Vidya, C. S. K. Raju, Peripheral layer viscosity on the stenotic blood vessels for Herschel-Bulkley fluid model, Inform. Med. Unlocked. 1(9) (2017), 161-165.

[14] D. S. Sankar, Perturbation analysis for pulsatile flow of Carreau fluid through tapered stenotic arteries, Int. J. Biomath. 9(4) (2016), 1650063.

[15] J. Singh, R. Rathee, Analysis of non-Newtonian blood flow through stenosed vessel in porous medium under the effect of magnetic field, Int. J. Phys. Sci. 6(10) (2011), 2497-2506.

[16] P. K. Suri, P. R. Suri, Effect of static magnetic field on blood flow in a branch, Indian J. Pure Appl. Math. 12(7) (1981), 907-918.

[17] E. E. Tzirtzilakis, A mathematical model for blood flow in magnetic field, Phys. Fluids. 17(7) (2005), 077103.

[18] G. Varshney, V. Katiyar, S. Kumar, Effect of magnetic field on the blood flow in artery having multiple stenosis: a numerical study, Int. J. Eng. Sci. Technol. 2(2) (2010), 967-982.

[19] V. B. Sreenivasa, A. Suresh Warke, Study of Two-Phase Unsteady Model of Blood Flow in a Tapered Stenosed Artery in the Presence of Externally Applied Transverse Magnetic Field, in: 2018 IEEE Punecon, IEEE, Pune, India, 2018: pp. 1–7.

[20] B. S. Veena, Effect of externally applied transverse magnetic field on unsteady flow of blood in tapered stenosed artery, Int. J. Eng. Adv. Technol. 8(6) (2019), 1398-1406.

[21] B. S. Veena, A. S. Warke, Study of blood flow in one half of cosine shaped stenosis in the presence of magnetic field, Int. J. Exp. Comput. Biomech. 3(2) (2015), 121-136.

[22] J. Venkatesan, D.S. Sankar, K. Hemalatha, Y. Yatim, Mathematical Analysis of Casson Fluid Model for Blood Rheology in Stenosed Narrow Arteries, J. Appl. Math. 2013 (2013), 583809.